Mitered Fractal Trees: Constructions and Properties

Tom Verhoeff *
Department of Mathematics and Computer Science
Eindhoven University of Technology
Den Dolech 2
5612 AZ Eindhoven, Netherlands
T.Verhoeff@tue.nl

Koos Verhoeff
Valkenswaard, Netherlands

Abstract

Tree-like structures, that is, branching structures without cycles, are attractive for artful expression. Especially interesting are fractal trees, where each subtree is a scaled and possibly otherwise transformed version of the entire tree. Such trees can be rendered in 3D by using beams with a polygonal cross section for the trunk and the branches. The challenge is to connect the beams at the branching points in such a way that the beam edges nicely meet. This is related to the miter joint, but does not necessarily involve ternary miter joints.

In this article, we explore a parameterized family of fractal trees that can be rendered with polygonal beams whose edges meet properly at the branching points. We present various constructions and analyze their mathematical properties. Some of these trees have been constructed as artwork in wood and bronze.

1 Introduction

Figure 1 : *Two mitered fractal trees as artwork, designed by Koos Verhoeff (left: bronze; right: wood)*

Figure 1 shows two tree-shaped artworks, whose designs date back to the late 1980s. The designs are fractal in nature, and involve beams with a rectangular (left) and square (right) cross section. The tree on the left looks wilder than the one on the right. Upon closer inspection, the tree on the right is highly structured, with the branches pointing in one of only six directions (three pairs of opposite directions).

We describe and analyze the designs of these two trees in the next two sections. In Section 4, we consider the general design problem of constructing mitered fractal trees from beams with a polygonal cross section, such that the longitudinal beam edges meet properly at each joint. Joints where edges meet properly also appear in [3, 4, 7]. It will turn out that there are several parameters that can be varied. This gives rise to a rich family of mitered fractal trees. We analyze mathematical properties of these trees in Section 5. Section 6 concludes the article.

2 $1 : \sqrt{2}$ Rectangular Beam

The first 3D fractal tree design (see Fig 2, left) is based on a beam with a $1 : \sqrt{2}$ rectangle as cross section. This beam type was well known to the authors, because when cut at $45°$ it yields a *square* cut face (see Fig 2, right, $P_1P_2P_3P_4$ at the bottom), giving rise to the so-called *skew miter joint*, where the cut face is not in the interior bisector plane of the angle spanned by the center lines of the beams joined [3].

The key observation for this tree design is that cutting that same beam *twice* at $45°$ from opposite sides, in a direction perpendicular to the bottom cut, yields a *roof* consisting of two squares (see Fig 2, right, $P_6P_7P_{10}P_9$ and $P_8P_5P_9P_{10}$ at the top). The squares of the roof are smaller than the square at the bottom by a factor $\sqrt{2}$. Thus, two smaller copies of the piece in Fig 2 (right) can be attached as *child* branches to that roof. In the first design, the right child points backward, and the left child points forward. The starting piece (trunk) is complemented by a *base* to level it off (see Fig 2, middle). The only parameter in this design is the length of each piece (P_3P_7). Make it too short (exact limits are not known), and the tree will self-intersect. Each subtree is a *scaled down copy* of the entire tree, which explains the fractal nature of the tree. In practice, only a finite number of *generations* is grown, as approximation of the limit fractal.

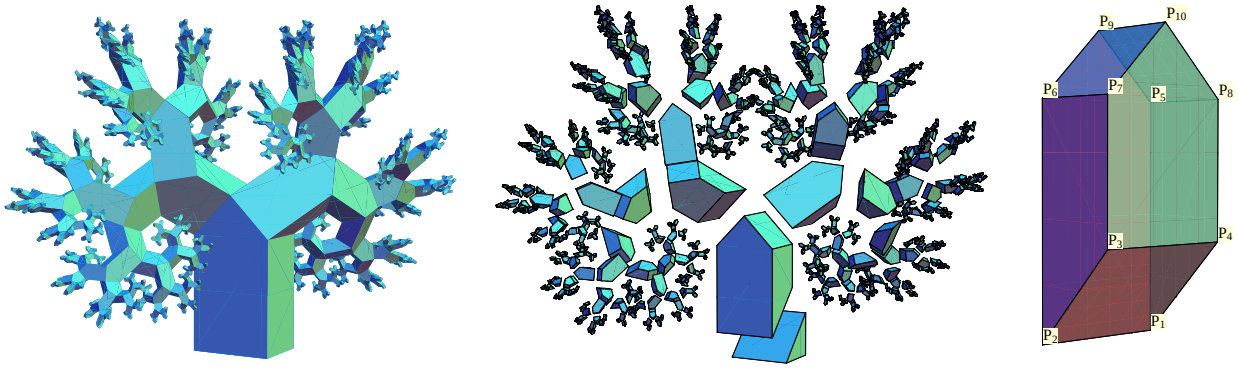

Figure 2 : *Mitered fractal tree from* $1 : \sqrt{2}$ *rectangular beams (left); exploded view (middle); piece (right)*

Note that the resulting joints are not *ternary miter joints*, as described and analyzed in [7]. In such a (regular) ternary miter joint, the cut faces are in the interior bisector planes, all cross sections are identical, and the center lines of the beams intersect in a point. None of these is the case here.

The angle between parent piece and child piece is $120°$, as is the angle between the two child pieces. Further mathematical details are presented in Section 5. Obvious variants of this tree are obtained by attaching the child pieces in different ways, as allowed by the square cut face. Figure 3 shows three variants.

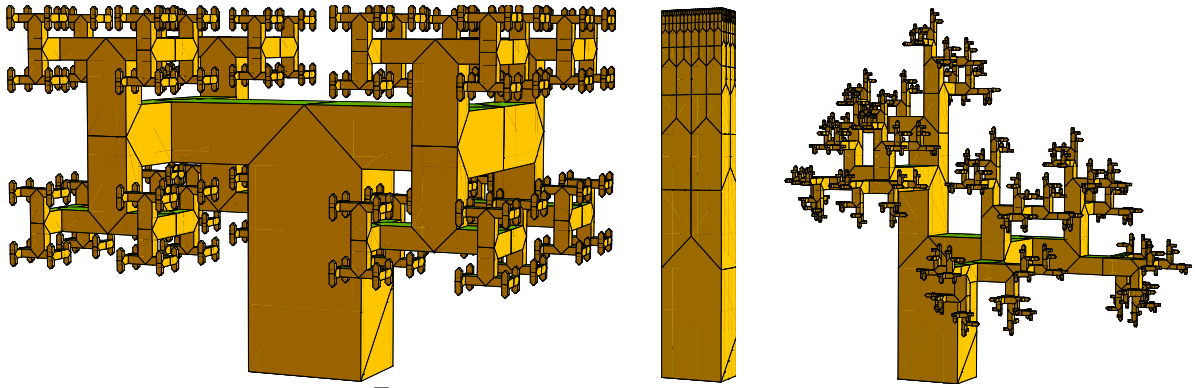

Figure 3 : *Variants on* $1 : \sqrt{2}$ *mitered fractal trees (left: side-side; middle: up-up; right: side-up)*

3 Square Beam

The second design (Fig. 4, right) arose as a variation on the first design, by *dualization*, that is, by swapping the shape of the cross section and the shape of the cut face. Take a beam with a square cross section. Cut it at $45°$ to obtain a $1 : \sqrt{2}$ rectangle as cut face (Fig. 4, left and middle, bottom cut). Similar to the preceding design, that beam can also be cut to have a roof consisting of two $1 : \sqrt{2}$ rectangles (Fig. 4, left, top cuts). This would yield a tree similar in shape to the first design (Fig. 5, left), but now with square beams.

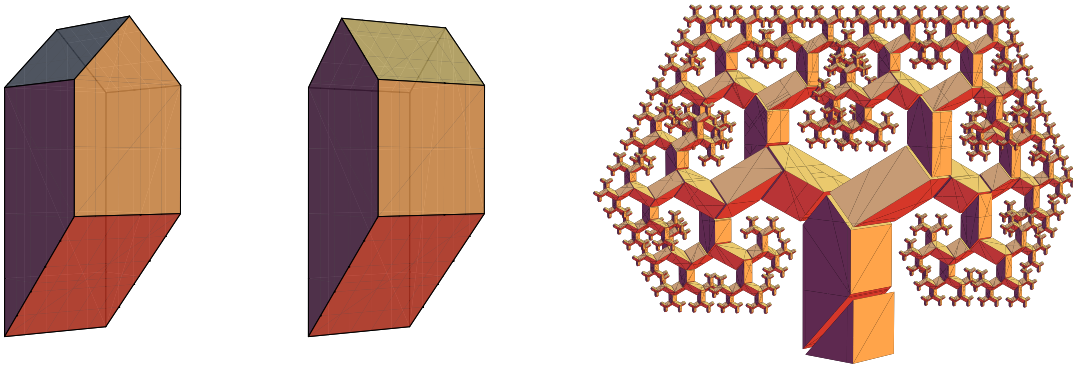

Figure 4 : *Square beams (left: orthogonal roof; middle: parallel roof); right: mitered fractal tree (exploded)*

In the first design, each branch could grow in one of four directions due to the square cut face. With the square beam, each branch can grow in one of only two directions, because the cut faces are rectangles. However, with a square beam, one can rotate the roof over $90°$ (see Fig. 4, middle), something that is not possible with the rectangular beam. This opens the door for new shapes. The second design, is based on a rotated roof and the child branches grow in opposite directions, where front-back alternates. To put the latter differently, each child subtree is a *mirrored* and scaled down copy of the parent tree.

Again, there are obvious variants; two are shown in Figure 5. On the left, an orthogonal roof with a shape similar to the first design (compare to Fig. 2, left). On the right, a parallel roof and non-mirrored subtrees, where branches have one of twelve directions.

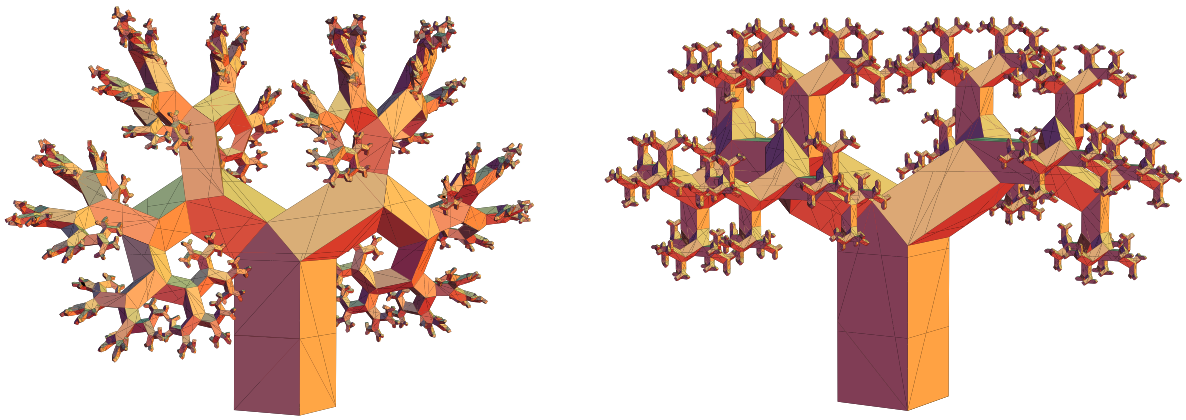

Figure 5 : *Variants with square beams (left: orthogonal roof; right: parallel roof, non-alternating)*

4 General Constructions

The designs described in the preceding two sections are *accidental*, in the sense that they are based on, what seem to be, special properties of the shapes involved ($1 : \sqrt{2}$ rectangles and squares). Over the years, we developed new insights, allowing us to describe more general constructions also leading to properly mitered fractal tree designs. Let us look at the constraints to be satisfied when designing a mitered fractal *binary* tree.

- The trunk has a *polygonal* cross section.
- Each subtree[1] is a *scaled down*, and possibly reflected, copy of the whole tree. Hence, the trunk and all branches have a *similar*[2] polygonal cross section.
- The longitudinal edges of the beams, representing the trunk and the branches, properly meet up at the three-way joints.

Of course, these are somewhat arbitrary requirements, but without constraints there would be little to investigate, since any branching structure would be constructible.

The first generalization concerns the design with the $1 : \sqrt{2}$ rectangular cross section and square cut faces. Consider a beam with a $1 : a$ rectangle ($a \geq 1$) cross section. Square cut faces can be obtained, by cutting at an appropriate angle, both at the base and at the roof. The base will expose an $a \times a$ square, and the roof will expose two 1×1 squares. Thus, the scale-down factor is a, implying that we need $a > 1$ for a genuine fractal, i.e., with a bounded limit. The roof will "flatten out" for $a = 2$; thus, we need $1 < a \leq 2$. Figure 6 (left) shows branches with various a, and (right) two corresponding trees, with extended trunks.

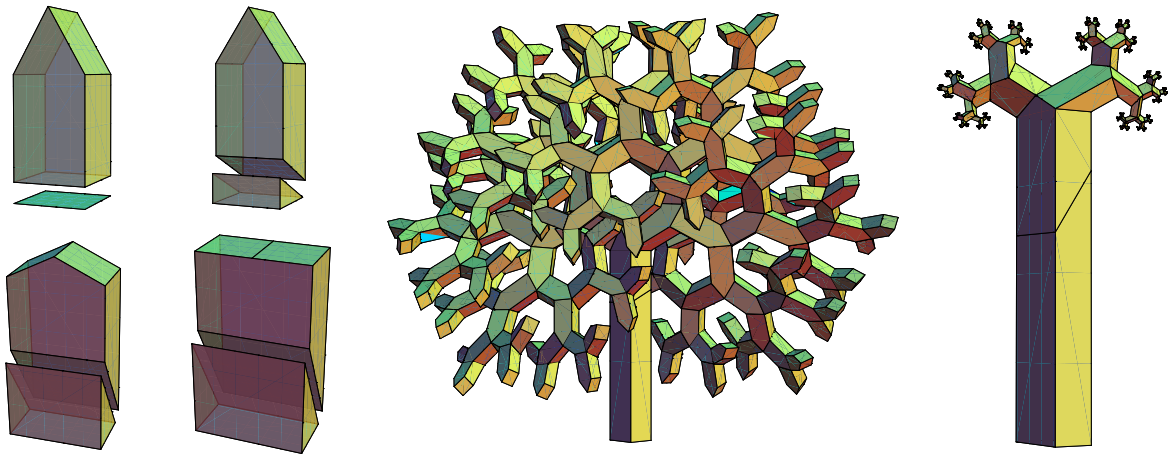

Figure 6: $1 : a$ *rectangular beams with square cut faces (left:* $a = 1,\ 1.1,\ 1.8,\ 2$*; right: trees with* $a = 1.1, 1.8$*)*

The second generalization concerns the design with the square cross section and $1 : \sqrt{2}$ rectangular cut faces. When cutting the square beam at an angle other than $45°$, we obtain a rectangular cut face with an aspect ratio other than $1 : \sqrt{2}$. The roof angle can be chosen to match that aspect ratio on its two panel halves. The roof can still be rotated over $90°$. In fact, even on a rectangular beam, the roof can be rotated over $90°$. But in that case, the roof angle must be adjusted as well, to make the two roof cuts match the base cut in aspect ratio.

Actually, there is no reason for the roof to be symmetric, with its ridge at the center. The ridge could be off center, and the slope of the left and the right panel could be chosen independently to tune the aspect

[1] A subtree consists of a branch and all smaller branches that grow from it.
[2] Similar is intended in the geometric sense: congruent after scaling.

ratio of both halves to coincide with that of the base cut. Figure 7 (left) shows an asymmetric piece from a $1 : \sqrt{2}$ rectangular beam and three square cut faces. The two roof panels are slanted at $60°$ (left) and $\arccos(\sqrt{2} - \cos(60°)) \approx 23.9°$ (right). Figure 9 (left) shows a tree with an asymmetric roof.

It is not even necessary that the cut faces be rectangles or squares. In general, when cutting a rectangular beam, the cut face is a parallelogram. By appropriately tilting the ridge, the cut faces can all be similar parallelograms. In Figure 7 (second from left), the trunk is again a $1 : \sqrt{2}$ rectangular beam. The ridge is slanted at $20°$ and the roof panels slope down at $30°$, giving rise to parallelograms with an aspect ratio (ratio between lengths of adjacent sides) $1 : 1.30$ and an angle of $80.15°$. The base cut face is also slanted at $20°$ and $30°$, yielding a similar parallelogram. In Figure 7 (second from right), that same beam is cut to yield three rhombi with angle of $72°$.

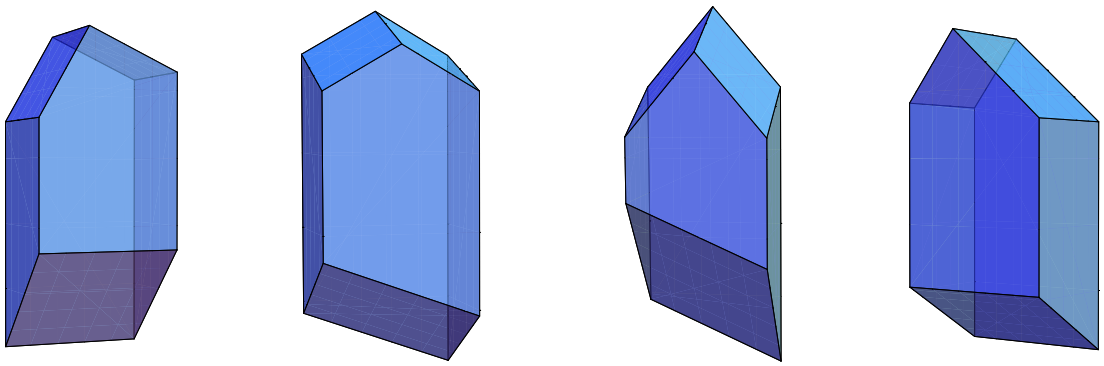

Figure 7: $1 : \sqrt{2}$ *rectangular trunk; left: asymmetric roof, all cut faces are square panels; second from left: roof with slanted ridge, all cut faces are similar parallelograms; second from right: rhombi as cut faces; right: rectangular cuts, roof halves similar but not congruent*

We now analyze the general situation of a polygonal (parent) beam that *splits* into two similar (child) beams at similar cut faces, where the two child beams only touch each other at the ridge. This contrasts to a ternary miter joint, where all pairs share a surface, rather than a line segment. If the cross section is a polygon with n vertices, then the beam has n longitudinal edges, and a cut face is also an n-gon (its shape is a *projection* of the cross section). The roof's ridge divides the n-gon into two halves, and can do so in three ways. It can meet zero, one, or two of the longitudinal beam edges. Supposing it meets k of them, each of the (similar) roof faces will have $(n - k)/2 + 2$ vertices. Since these faces are similar to the whole, we have $(n - k)/2 + 2 = n$ and, hence, $n = 4 - k$. In summary,

- for $k = 0$, the cross section is a *quadrangle*;
- for $k = 1$, the cross section is a *triangle*;
- for $k = 2$, the cross section is a *strip* (a degenerate case, leading to 2D rather than 3D beams).

We will only deal with the case of a rectangular cross section here. Consider the $a : b$ rectangular cross section, where the base cut is a parallelogram that slopes up along side a at angle α and along side b at angle β. That parallelogram has aspect ratio ρ and angle ϕ between adjacent sides satisfying

$$\rho = a \cos\beta : b \cos\alpha \tag{1}$$

$$\cos\phi = \sin\alpha \sin\beta \tag{2}$$

Note that $\phi = 90°$, i.e., the cut is rectangular, when either $\alpha = 0$ or $\beta = 0$, regardless of the other angle. If neither α nor β equals zero, then ϕ depends on both α and β, and the cut is not rectangular.

Two parallelograms are similar when they have the same aspect ratios *and* the same angles. Since the two halves of the roof share the ridge, they have the same slope in that direction. In order to be similar, their

other slopes must be equal (in absolute value, i.e., disregarding signs) as well, *unless* the ridge is horizontal (slope 0). There are two ways in which these two halves can be mapped to each other:

1. The sides at the ridge are mapped to each other; in this case, the other sides must be equal, and thus the ridge must be *centered* (*unless* the ridge is horizontal) and the halves are *congruent*; see Fig. 8 (left).
2. The sides at the ridge are *not* mapped to each other; in this case, the two halves are *not congruent* (*unless* the aspect ratio is one); see Fig. 7 (right) and 8 (right).

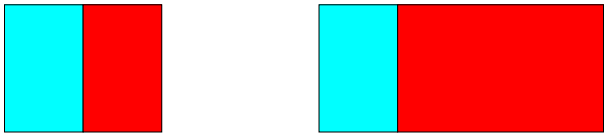

Figure 8 : *The two ways that two roof halves (cyan and red) can share a side and be similar*

This completes the classification of possibilities for a rectangular cross section.

There is yet another way to generalize the branching process, viz. from binary trees to n-ary trees, where each parent "grows" $n > 2$ children. Figure 9 (right) shows a ternary tree with a rectangular cross section, where the roof consists of three similar rectangular panels. The panels of the roof can be organized in many ways. We will not pursue this further here.

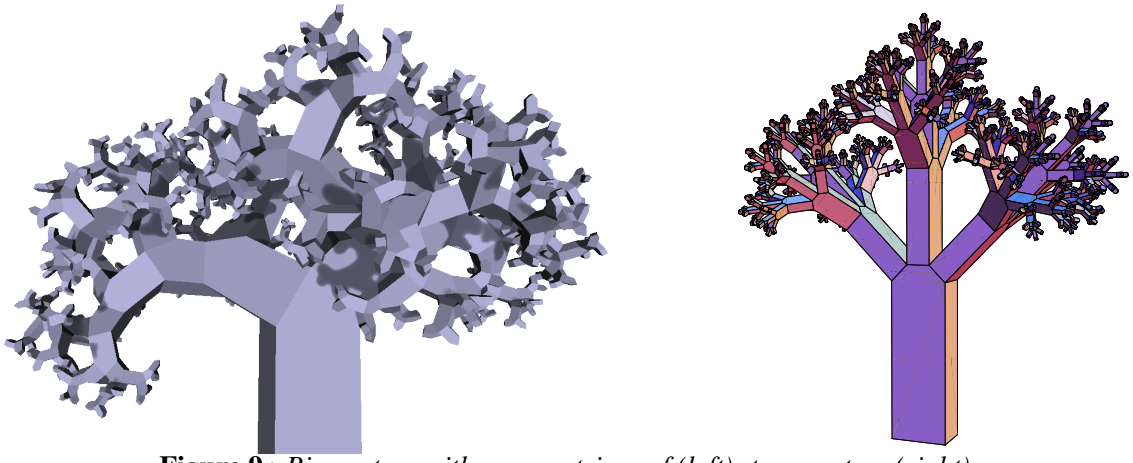

Figure 9 : *Binary tree with asymmetric roof (left); ternary tree (right)*

5 Mathematical Properties

In this section, we address various mathematical properties of the mitered fractal trees presented in the preceding sections. In particular, we will look at their fractal dimension, self-intersection, symmetries, total branch cross section, and branch directions.

In a fractal object, the number N of self-similar copies in each next generation and the scale-down factor f ($f > 1$) between generations are related by a power law: $N \propto f^D$, where D is the *fractal dimension* of the fractal object. Given N and f, one can determine the fractal dimension D from

$$D = \frac{\log N}{\log f} \tag{3}$$

Consider the fractal tree of Section 2 in Figure 2 (left). In the limit, this fractal tree consists of a trunk to which are attached two copies of the entire tree scaled down by a factor $\sqrt{2}$. Thus, we have $N = 2$ and

$f = \sqrt{2}$. Its fractal dimension is 2, since $\log \sqrt{2} = \frac{1}{2} \log 2$. A tree may seem to be a one-dimensional object, since it is constructed from one-dimensional branches, but this tree, in the limit, is actually two-dimensional. The fractal tree of Section 3 in Figure 4 (right) also has fractal dimension $D = 2$.

The general constructions of Section 4 give rise to other fractal dimensions. For instance, the first generalization has scale-down factor a and, hence, $D = \log 2 / \log a$. For the tree in Figure 6, with $a = 1.1$ we get $D = 7.27$ (this tree self-intersects, since $D > 3$) and with $a = 1.8$ we get $D = 1.18$. For $a = \sqrt[3]{2} \approx 1.26$, we would get $D = 3$, i.e., a space-filling tree.

In general, it is not easy to determine whether a tree *self-intersects*. If its fractal dimension exceeds three, then it is reasonably certain that the tree self-intersects (in the limit). But this is possibly also the case with a fractal dimension below three. Self-intersection is relevant when constructing these trees from, say, wooden beams. However, for 3D-printing it does not matter.

The two trees described in §2–3 are not *mirror-symmetric*, but they have a $180°$ *rotational symmetry* (i.e., of order 2). The two trees on the left in Figure 3 also have that rotational symmetry of order 2 and they are mirror-symmetric, but they are somewhat 'dull'. We have not been able to find 'nice' binary trees with these constructions that are mirror symmetric. Note that the ternary tree of Figure 9 (right) is mirror symmetric. The general constructions with non-centered or sloping roof ridges often give rise to asymmetric trees; see Figure 9 (left).

Leonardo da Vinci observed in one of his notebooks that "All the branches of a [natural] tree at every stage of its height when put together are equal in thickness to the trunk" [2, item 394]. Or, phrased differently by Eloy in [1], "the *total cross section of branches* is conserved across branching nodes". Eloy recently put forward the theory that this property evolved to help trees withstand wind-induced stresses. It turns out that the fractal trees in §2–3 satisfy Leonardo's tree rule: the scale-down factor is $\sqrt{2}$, thus the area scales by a factor 2, and each branch splits into two child branches.

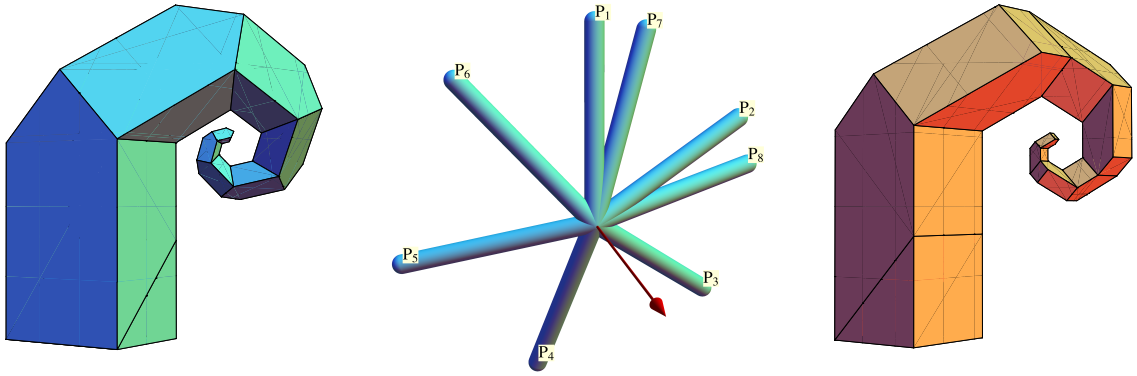

Figure 10 : *Tree of Fig. 2 with right child branches only (left); its branch directions translated to the origin; red arrow marks the helix axis (middle); tree of Fig. 4 with right child branches only*

Finally, we analyze the *directions of branches* in mitered fractal trees. Figure 10 (left, right) shows the degenerate unary trees obtained from the trees in §2–3 by including only the right child branches. These paths can be described by the motion of a 3D turtle [6], which moves, turns, and rolls. Such helical paths were analyzed in [8]. The turn angle for these trees is $60°$, giving rise to a $120°$ between parent and child branches. In the second design, the roll angle is 0, thereby explaining that only six branch directions occur. The first design, however, involves a roll of $19.47°$ (angle between adjacent angle-spanning planes). When all the branches are reduced to tubes and translated to the origin, they lie on a cone, rather than a disc (see Fig. 10, middle). According to [8], the projected angle θ between successive branches is related to the turn angle ϕ and roll angle ψ by $\cos(\theta/2) = \cos(\phi/2)\cos(\psi/2)$. The branches point in a finite number of directions if and only if the angle θ is a rational multiple of $360°$. In the first design, we have $\theta \approx 62.80°$.

6 Conclusion

We started by presenting two specific designs for fractal trees constructed from polygonal (rectangular and square respectively) beams, where the longitudinal edges properly meet at the branching joints. Next we analyzed general designs, giving rise to a rich family of constructions. In particular, we showed that this kind of joint is only possible for cross sections with at most four vertices, and we classified all design options for a rectangular cross section.

Joining two beams with the same cross section such that longitudinal edges properly meet results in a *miter joint* [4]. A comprehensive treatment appears in [3], where *regular* and *skew* miter joints are distinguished. The first design was inspired by skew miter joints. We pointed out how the joints where child branches "grow" from a parent branch differ from the ternary miter joints in [7]. In our mathematical analyses, we focused on symmetries and branch directions.

There are several unexplored possibilities, such as (1) general quadrangles as cross section, (2) n-ary trees with $n > 2$, (3) constructing longer tree fragments before repeating a back/front pattern (e.g., first and second right child points to the back, third and fourth right child point to the front, and only then the pattern repeats), which is related to [5], and (4) child branches that share a surface (as happens in ternary miter joints) but where the cross section nevertheless scales down (which is not the case in ternary miter joints).

Acknowledgments Koos Verhoeff designed all shown artwork. The bronze fractal tree (Fig. 1, left) was constructed by Anton Bakker and Kevin Gallup, and the wooden fractal tree (Fig. 1, right) was constructed by Hans de Koning. The illustrations were made with *Mathematica*.

References

[1] C. Eloy. "Leonardo's Rule, Self-Similarity, and Wind-Induced Stresses in Trees." *Physical Review Letters* 107, 258101 (2011).

[2] J. P. Richter (Ed.). *The Notebooks of Leonardo da Vinci, Vol. I*. Dover, 1970.
URL: `www.sacred-texts.com/aor/dv` (accessed 30 Jan. 2012)

[3] T. Verhoeff, K. Verhoeff. "The Mathematics of Mitering and Its Artful Application", *Bridges Leeuwarden: Mathematical Connections in Art, Music, and Science, Proceedings of the Eleventh Annual Bridges Conference, in The Netherlands*, pp. 225–234, July 2008.

[4] T. Verhoeff. "Miter Joint and Fold Joint". From *The Wolfram Demonstrations Project*, `demonstrations.wolfram.com/MiterJointAndFoldJoint` (accessed 26 January 2010).

[5] T. Verhoeff, K. Verhoeff. "Regular 3D Polygonal Circuits of Constant Torsion", *Bridges Banff: Mathematics, Music, Art, Architecture, Culture, Proceedings of the Twelfth Annual Bridges Conference, in Canada*, pp.223–230, July 2009.

[6] Tom Verhoeff. "3D Turtle Geometry: Artwork, Theory, Program Equivalence and Symmetry". *Int. J. of Arts and Technology*, **3**(2/3):288–319 (2010).

[7] T. Verhoeff, K. Verhoeff. "Branching Miter Joints: Principles and Artwork". In: George W. Hart, Reza Sarhangi (Eds.), *Proceedings of Bridges 2010: Mathematics, Music, Art, Architecture, Culture*. Tessellations Publishing, pp.27–34, July 2010.

[8] T. Verhoeff, K. Verhoeff. "From Chain-link Fence to Space-spanning Mathematial Structures". In: Reza Sarhangi and Carlo Séquin (Eds.), *Proceedings of Bridges 2011: Mathematics, Music, Art, Architecture, Culture*. Tessellations Publishing, pp.73–80, July 2011.